JOM, Vol. 69, No. 12, 2017
DOI: 10.1007/s11837-017-2583-4

Microstructure and Tensile Properties of Ti-48Al-2Cr-2Nb Rods Additively Manufactured by Selective Electron Beam Melting

J. WANG,[1] K. YANG,[1] N. LIU,[1] L. JIA,[1] G.Y. YANG,[1] and H.P. TANG[1,2]

1.—State Key Laboratory of Porous Metal Materials, Northwest Institute for Nonferrous Metal Research, Xi'an 710016, China. 2.—e-mail: thpfys@126.com

A batch of Ti-48Al-2Cr-2Nb (at.%) rods (diameter 15 mm, height 70 mm) has been additively manufactured by selective electron beam melting (SEBM), and a detailed assessment made of their chemical composition, density before and after hot isostatic pressing, microstructure, and tensile properties. The microstructure of the SEBM Ti-48Al-2Cr-2Nb in as-built condition was composed of fine equiaxed grains consisting of lamellar γ/α_2 colonies and a small amount of coarse γ grains. Owing to the fine and dense microstructure (relative density 99.8%), the tensile yield strength of the SEBM Ti-48Al-2Cr-2Nb reached 555 ± 11.3 MPa, while the tensile elongation reached 0.94 ± 0.06%. The oxygen content changed from 0.089 wt.% in the feedstock powder to 0.093% in the as-built alloy within the range of measurement error. However, the content of Al decreased from 33.8 wt.% in the feedstock powder to 32.3 wt.% in the as-built samples. Observations of various microstructure features are discussed.

INTRODUCTION

Additive manufacturing (AM) offers an attractive cost-effective route for manufacture of γ-TiAl components, with unrivaled advantages in terms of design freedom, shape formation, and reduced lead time and materials utilization. Selective electron beam melting (SEBM) is a powder-bed-based AM technology that is particularly suited to AM of γ-TiAl components, because the powder bed can be kept at a substantially higher temperature (up to 1100°C), enabling effective release of thermal stress accumulated during AM, thereby preventing crack formation.[1]

Several studies have reported on SEBM γ-TiAl alloys.[2–7] Murr et al.[2] and Biamino et al.[3] reported that Ti-48Al-2Cr-2Nb (in at.% throughout the paper) samples with residual porosity below 2% could be achieved by SEBM. Schwerdtfeger et al.[4] found that a wide range of microstructures from lamellar to massively transformed γ could be realized by varying SEBM parameters. However, to the authors' best knowledge, only a few studies[6,7] have been published on the tensile properties of SEBM TiAl alloys in as-built state, which limits comprehension of the SEBM process of these alloys. The work presented herein was carried out to fill this gap in literature on SEBM TiAl alloys.

EXPERIMENTAL PROCEDURES

Materials and SEBM Processes

Spherical Ti-48Al-2Cr-2Nb powder (Fig. 1a) in the size range of 42–124 μm supplied by Arcam was used; its composition is listed in Table I. Internal small voids were found in some powder particles, as shown in Fig. 1b.

An array of nine Ti-48Al-2Cr-2Nb rods with dimensions of Φ15 mm × 70 mm was built using an Arcam A2 machine; the main processing parameters are summarized in Table II. All samples were built vertically on stainless-steel substrate (100 mm × 100 mm × 10 mm) preheated to 1050°C. During SEBM,the building chamber was kept at vacuum at 0.01 Pa, adjusted by using helium as regulating gas. After building, selected as-built samples were subjected to hot isostatic pressing (HIP) at 1260°C for 4 h under 150 MPa to obtain fully dense samples.

(Published online September 18, 2017)

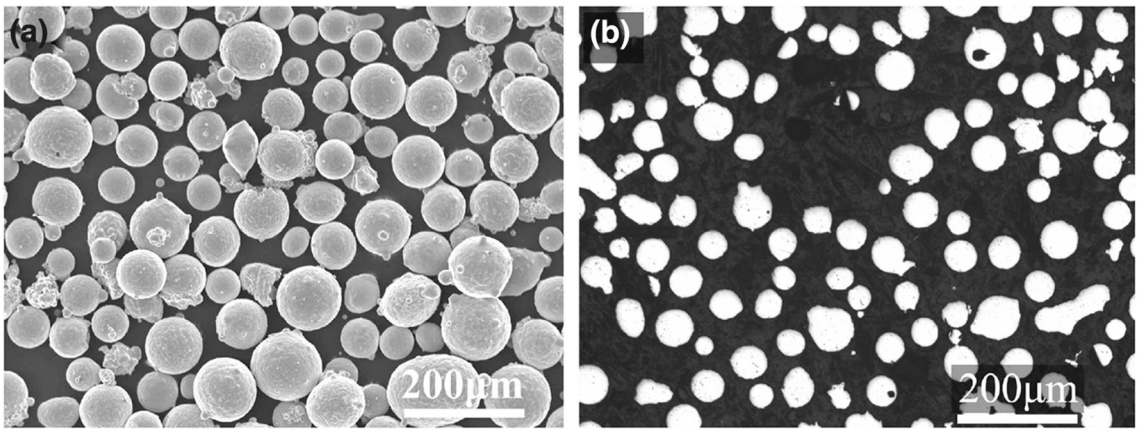

Fig. 1. SEM and optical images of as-received gas-atomized Ti-48Al-2Cr-2Nb powder: (a) typical powder morphology and (b) small voids in powder particles.

Table I. Composition of as-received Ti-48Al-2Cr-2Nb powder and as-built rods

	Composition (wt.%)						
	Ti	**Al**	**Cr**	**Nb**	**O**	**C**	**N**
As-received powder	Bal.	33.80	2.40	5.00	0.089	0.006	0.007
As-built rods	Bal.	32.30	2.45	4.46	0.093	0.007	0.008

Table II. SEBM parameters used for building Ti-48Al-2Cr-2Nb rods

Process	**Basic parameters**	**Value**
Application of powder	Layer thickness	180 μm
	Preheating temperature	1050°C
Preheating	Beam current	46 mA
	Beam scanning speed	12,000 mm/s
Layer melting	Beam current	12–17 mA
	Beam scanning speed	1600 mm/s

Characterization and Tensile Testing

The density of the rods was determined using the Archimedes method according to ISO 2738:1999. Samples for metallographic analysis were cut along the building direction. They were ground, polished, and etched using Kroll's reagent (3 ml HF, 5 ml HNO_3, and 100 ml H_2O) for characterization by optical microscopy (OM). X-ray diffraction (XRD) analysis was performed on a Bruker D8 Advance diffractometer at 40 kV using Cu K_α radiation (wavelength $\lambda_{k\alpha 1}$ = 1.54060 Å).

Standard tensile specimens with gauge dimensions of Φ5 mm × 25 mm were machined from as-built rods according to ISO 6892-1:2009. Tensile testing was performed using an Instron model 5985 (Instron Corporation, Norwood, MA) with constant crosshead speed of 0.1 mm/min.

RESULTS AND DISCUSSION

Chemical Composition and Density

Owing to the high-vacuum chamber used in SEBM, the aluminum content decreased from 33.83 wt.% to 32.30 wt.% (Table I) because of volatilization. However, there was essentially no pick-up of oxygen, nitrogen or carbon (Table I), which is important because of the high sensitivity of γ-TiAl to impurities.[8] It is likely that the aluminum vapor helped to minimize the oxygen content in the chamber during SEBM.

The as-built samples reached density of 3.971 ± 0.004 g/m^3, comparable to that of Ti-48Al-2Cr-2Nb ingots (3.97 g/m^3, GfeMetalle und Materialien GmbH, Germany).[9] In addition, lack of fusion and small void defects were occasionally observed in

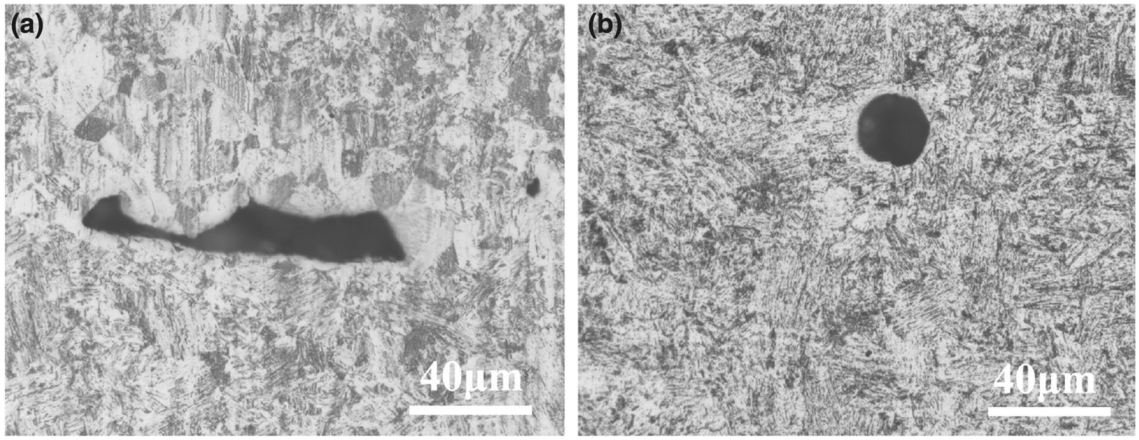

Fig. 2. Defects occasionally observed in as-built Ti-48Al-2Cr-2Nb alloy samples: (a) lack of fusion and (b) small voids.

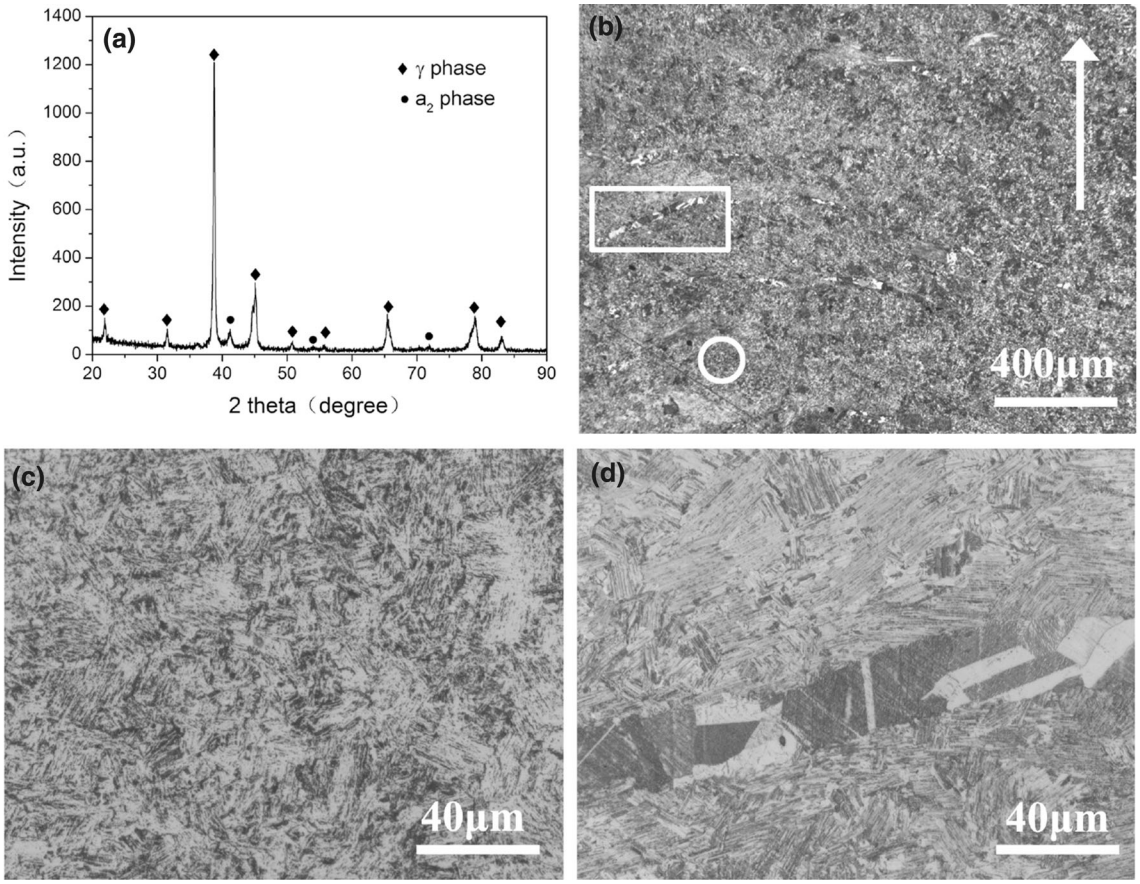

Fig. 3. (a) XRD spectrum and (b) optical microstructure of SEBM Ti-48Al-2Cr-2Nb (build direction indicated by arrow); (c, d) details of areas marked by circle and rectangle in (b), respectively.

as-built samples, as shown in Fig. 2a and b. However, no such defects were observed after HIP, suggesting that fully dense samples (3.979 ± 0.007 g/m^3) were obtained after HIP. Accordingly, the relative density of the SEBM Ti-48Al-2Cr-2Nb in this study reached 99.8%.

Microstructure

According to the XRD spectrum of the SEBM Ti-48Al-2Cr-2Nb alloy (Fig. 3a), γ-TiAl and α_2-Ti_3Al were the predominant phases in the as-built samples. Figure 3b, c, and d shows the longitudinal

microstructure of the as-built samples. In general, columnar grains are easy to form in low-solute-content alloys due to the large thermal gradient in the SEBM melt pool. However, the SEBMTi-48Al-2Cr-2Nb alloy mainly consisted of fine equiaxed grains, as shown in Fig. 3b. In addition, closer observations at high magnifications revealed that the microstructure was inhomogeneous. Most areas marked by a circle in Fig. 3b exhibited fine lamellar $\gamma + \alpha_2$ structure with colony size smaller than 40 μm, as shown in Fig. 3c, whereas those marked by a rectangle in Fig. 3b exhibited coarser γ grain structure (Fig. 3d).

Tensile Properties

Figure 4 shows tensile stress–strain curves of SEBM Ti-48Al-2Cr-2Nb in as-built state. The tensile property results are summarized in detail in Table III, together with reference data for the tensile properties of Ti-48Al-2Cr-2Nb processed by other methods. SEBM Ti-48Al-2Cr-2Nb alloy obtained in this work showed the highest tensile yield strength (555 ± 11.31 MPa) and tensile strength (603 ± 18.38 MPa). Although the tensile elongation value (0.94 ± 0.06%) was lower than achieved by HIP[10] and casting,[11] it was higher than the values for SEBM Ti-48Al-2Cr-2Nb reported by Franzen et al.[6] and Chen et al.[7] and similar to that of SEBM Ti-48Al-2Cr-2Nb postprocessed by HIP and heat treatment.[3]

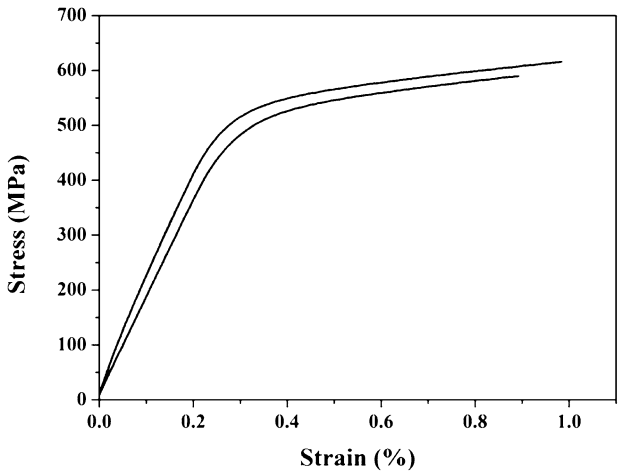

Fig. 4. Tensile stress–strain curves of SEBM Ti-48Al-2Cr-2Nb alloy samples

DISCUSSION

The lack-of-fusion defects can be attributed to the nonoptimized process. Murr et al.[2] and Biamino et al.[3] reported that the small voids were due to internal gas pores in the as-received powder particles. To clarify this issue, selected HIP-processed samples were held isothermally at 1300°C for 4 h, followed by furnace cooling. The resulting density (3.980 ± 0.005 g/m^3) was the same as that of the HIP-processed sample (3.979 ± 0.007 g/m^3). No small voids resurfaced due to potential expansion during isothermal holding according to OM observations. In other words, the small voids observed in the as-built samples may not arise from gas bubbles in the as-received powder; Rather, they could be caused by the evaporation of 1.53 wt.% Al during SEBM.

Unlike SEBM of Ti-6Al-4 V, which leads to prominent columnar prior-β grains, the SEBM Ti-48Al-2Cr-2Nb alloy exhibited fine equiaxed grain structure, consistent with other studies.[2,3,5] This can be attributed to the high cooling rate in the SEBM process,[12,13] as well as the high solute content, which contributes to constitutional undercooling-driven equiaxed grain formation.[14] Fine lamellar γ/α_2 microstructures were found within the equiaxed grains in this study. It has been reported that TiAl alloys with fine lamellar γ/α_2 microstructure can be obtained by fast cyclic heat treatment.[15,16] On this basis, the formation of these fine lamellar γ/α_2 microstructures can be interpreted based on the in situ heat treatment process during SEBM. In a typical SEBM process, the as-solidified Ti-48Al-2Cr-2Nb will always be heat-affected by neighboring lines and layers, and the temperature could rapidly exceed the α transition or eutectoid transition temperature more than once. This could lead to formation of the fine lamellar γ/α_2 microstructure.

Table III. Tensile properties of Ti-48Al-2Cr-2Nb in different conditions

Processing	YS (MPa)	UTS (MPa)	EL (%)	Microstructure	References
SEBM	555 ± 11.31	603 ± 18.38	0.94 ± 0.06	Lamellar	This study
SEBM	–	337.8	0.18	Lamellar	Ref. 6
SEBM	–	503 ± 18	0	Equiaxed γ	Ref. 7
SEBM + HIP	370	430	1.1	Equiaxed γ	Ref. 3
SEBM + HIP + HT	382 ± 11	474 ± 23	1.3 ± 0.3	Duplex	Ref. 7
SEBM + HIP + HT	350	470	1.1	Duplex	Ref. 3
HIP	370	460	2	Duplex	Ref. 10
Cast + HIP + HT	329	465	2.4	Duplex	Ref. 11

YS yield strength, *UTS* ultimate tensile strength, *EL* elongation, *HT* heat treatment.

It has been reported that the tensile strength of dual-phase TiAl alloys is inversely proportional to the grain size according to the Hall–Petch relationship.[8] The high yield strength and tensile strength of the SEBM Ti-48Al-2Cr-2Nb produced in this research can be attributed to the fine microstructure shown in Fig. 3. In terms of tensile ductility, many studies have found that duplex microstructure of fine lamellar colonies and equiaxed γ grains results in Ti-48Al-2Cr-2Nb alloy with the best tensile ductility.[8] In this study, the SEBM Ti-48Al-2Cr-2Nb exhibited fine lamellar structure rather than duplex microstructure. This could be the reason why their tensile elongation is lower than that of Ti-48Al-2Cr-2Nb produced by casting or powder metallurgy (PM), which has duplex microstructure.

CONCLUSION

- SEBM is capable of fabricating Ti-48Al-2Cr-2Nb rods with relative density of 99.8%. Lack-of-fusion defects and small voids were observed occasionally in the as-built samples but could be healed by HIP at 1260°C for 4 h under 150 MPa.
- The content of Al decreased from 33.8 wt.% in the feedstock powder to 32.3 wt.% in the as-built samples.
- The microstructure of the SEBM Ti-48Al-2Cr-2Nb consisted of fine equiaxed grains, which further contained lamellar γ/α_2 colonies, and a small amount of coarse γ grains.
- SEBM Ti-48Al-2Cr-2Nb exhibited excellent tensile properties, including yield strength of 555 ± 11.3 MPa, tensile strength of 603 ± 18.38 MPa, and tensile elongation of 0.94 ± 0.06%.

ACKNOWLEDGEMENTS

This work is supported by Shaanxi Province Science and Technology Project (Grant No. 2015KTCQ01-60).

REFERENCES

1. H.P. Tang, G.Y. Yang, W.P. Jia, W.W. He, S.L. Lu, and M. Qian, *Mater. Sci. Eng. A* 636, 103 (2015).
2. L.E. Murr, S.M. Gaytan, A. Ceylan, E. Martinez, J.L. Martinez, D.H. Hernandez, B.I. Machado, D.A. Ramirez, F. Medina, S. Collins, and R.B. Wicker, *Acta Mater.* 58, 1887 (2015).
3. S. Biamino, A. Penna, U. Ackelid, S. Sabbadini, O. Tassa, P. Fino, M. Pavese, P. Gennaro, and C. Badini, *Intermetallics* 19, 776 (2011).
4. J. Schwerdtfeger and C. Körner, *Intermetallics* 49, 29 (2014).
5. G. Baudana, S. Biamino, B. Klöden, A. Kirchner, T. Weißgärber, B. Kieback, M. Pavese, D. Ugues, P. Fino, and C. Badini, *Intermetallics* 73, 43 (2016).
6. http://publications.lib.chalmers.se/records/fulltext/127716.pdf. Accessed 9 August 2017.
7. W. Chen, Y. Yang, L.L. Liu, Z.Y. Chen, and D. Liu, *Aeronaut. Manuf. Technol.* 40, 37 (2017).
8. K. Kothari, R. Radhakrishnan, and N.M. Wereley, *Prog. Aerosp. Sci.* 55, 1 (2012).
9. http://www.gfe.com/fileadmin/user_upload/pdfs/Produktspezifikationen_Titanium_Aluminides/PDB_gamma-TiAl_48-2-2-Ingot.pdf. Accessed 15 June 2017.
10. C. Tönnes, J. Rösler, R. Baumann, and M. Thumann, *Structural Intermetallics* (Warrendale: TMS, 1993), p. 241.
11. T.G. Kelly, M.C. Juhas, and S.C. Huang, *Scr. Metall.* 29, 1409 (1993).
12. M. Qian, W. Xu, M. Brandt, and H.P. Tang, *MRS Bull.* 41, 775 (2016).
13. C. Körner, *Int. Mater. Rev.* 61, 361 (2016).
14. M. Qian, P. Cao, M.A. Easton, S.D. McDonald, and D.H. StJohn, *Acta Mater.* 58, 3262 (2010).
15. J.N. Wang, J. Yang, Q.F. Xia, and Y. Wang, *Mater. Sci. Eng.* A329–331, 118 (2002).
16. A. Kościelna and W. Szkliniarz, *Mater. Charact.* 60, 1158 (2009).